

Supporting Information

Mesoporous Ternary Transition Metal Oxide Nanoparticles Composite for High-Performance Asymmetric Supercapacitor Devices with High Specific Energy

Nourhan M. Deyab ^{a, b, 1}, Manar M. Taha ^{a, 1}, and Nageh K. Allam ^{a*}

^aEnergy Materials Laboratory, School of Sciences and Engineering, The American University in Cairo, New Cairo 11835, Egypt.

^bPhysical Chemistry Department, National Research Centre, Dokki, Giza, Egypt.

* Corresponding Author: nageh.allam@aucegypt.edu

Materials and reagents:

Ti-0.3Mo-0.8Ni foil with 99% purity were purchased from Firmetal Co. Ltd (1.0 cm × 1.0 mm × 0.5 mm). Urea was purchased from Alfa Aesar and extra purified through recrystallization in absolute ethyl alcohol. Also, Ethylenediaminetetraacetic acid disodium salt and polyvinylidene difluoride powder (PVDF) were obtained from Alfa Aesar. Potassium sulphate (K₂SO₄) and dimethyl formamide (DMF) were purchased from Sigma Aldrich. Perchloric acid (HClO₄) and hydrochloric acid (HCl) were purchased from Honeywell. Carbon black and graphite sheets with 0.3 mm thickness were obtained from Xinruida, China. All the materials used were reagents of analytical grade without any further purification. Deionized water (DI) was prepared by an ultrapure water system using Millipore Direct-Q3 with UV. Slandered calomel electrode from obtained from CHI.

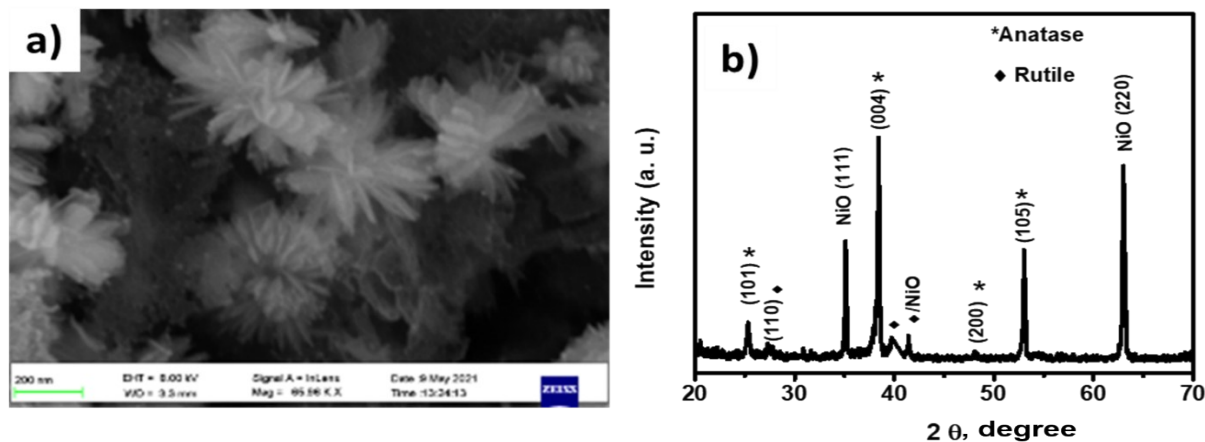


Figure S1. a) Top-view FESEM image of the resulted structures upon breakdown anodization of Ti-Mo-Ni sheet in 0.2 M HClO₄ aqueous electrolyte at 20 V and b) the corresponding XRD pattern.

Figure S2b depicts the XRD pattern of the synthesized Ti-Mo-Ni-O, revealing characteristic diffraction peaks at $2\theta = 25.6^\circ$, 38.2° , 48.1° , and 53.07° that can be assigned to the (101), (004), (200), and (105) planes of anatase TiO₂ (ICDD Card No. 01-071-1168), respectively [1–3]. Additionally, some diffraction peaks characteristic of NiO were also observed at $2\theta = 35.5^\circ$ and 63.1° that can be ascribed to the crystalline planes of (111) and (220), respectively. Moreover, rutile TiO₂ peaks were recorded at $2\theta = 27.5^\circ$ and 39.9° that are characteristic of the crystalline planes of (110) and (111), respectively. The peak at 41.4° could be interference between NiO (200) and rutile (210) [1]. Note that no diffraction peaks were detected for Mo oxides, suggesting the incorporation of their ions into the TiO₂ lattice or may be due to their very small percentage compared to Ti [4].

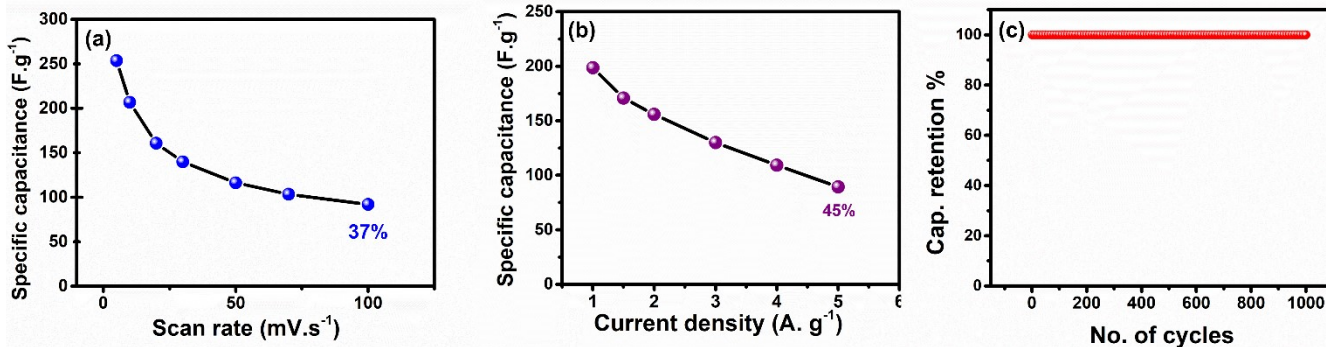


Figure S2. Rate capability of Ti-Mo-Ni-O electrode from (a) CV, (b) GCD, and (c) three-electrode stability test at 50 mV/s.

Synthesis of mesoporous doped carbon (MPDC):

A typical direct pyrolysis method was applied to a certain amount of EDTA-disodium salt. It was thermally treated in a ceramic boat into a horizontal thermo-scientific tube in a tube furnace at 800 °C for 2 hours at each temperature, under Argon gas flow, with a ramping rate 5 °C.min⁻¹ for both heating and cooling processes. Then, the obtained black residue product was firstly washed by diluted 0.5 M HCl followed by deionized water washing until a neutral pH was achieved. Finally, the sample was filtrated carefully, then dried overnight at 80 °C. The produced mesoporous nitrogen-doped carbons here are denoted as MPDC.

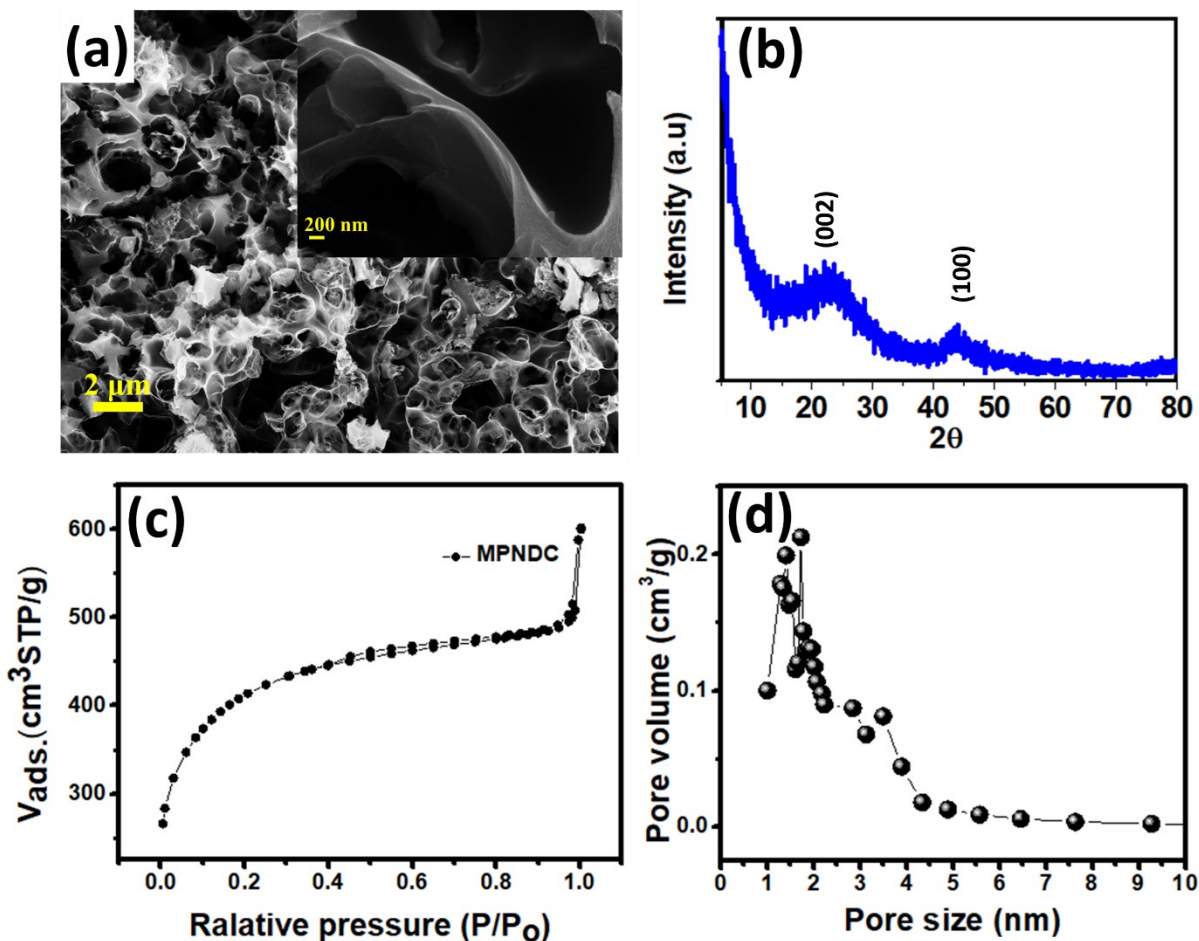


Figure S3. a) SEM image inset; high magnification, (b) XRD pattern c) N₂ adsorption-desorption, and d) pore size distribution of the MPDC materials.

Figure S3a depicts the SEM image of the hierarchical interconnected carbon channels of the MPDC. Also, **Figure S3b** displays the corresponding XRD pattern, which exhibited (002) and (100) diffraction peaks. These two peaks are generally related to the stacking of graphene interlayers and the ordered graphene domains, respectively. Furthermore, the surface area analysis was investigated using N₂-adsorption-desorption isotherm as shown in **Figure S3c**. The isotherms exhibit a sharp increase of nitrogen sorption at low pressure ($P/P_0 < 0.2$), which confirms the existence of micropores. Also, a hysteresis loop was observed at high relative pressure ($P/P_0 > 0.3$), revealing the presence

of mesoporous structure. Based on the IUPAC classification, all the samples show type-IV sorption isotherm behavior with H4-type hysteresis loops. Additionally, the desorption BJH pore size distribution (PSD) plots confirmed the coexistence of microporous and mesoporous structures of ~ 1.6 and ~ 3.5 nm as shown in **Figure S3d**.

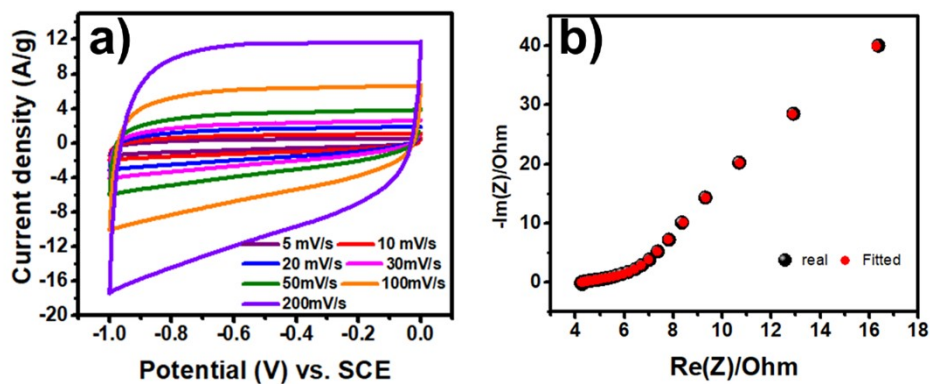


Figure S4. (a) CVs and (b) PEIS of the negative electrode.

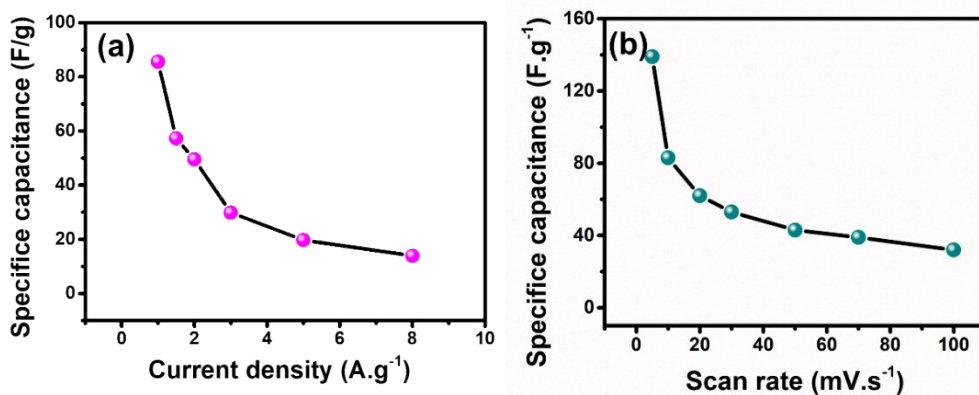


Figure S5. Rate capability of ASC device.

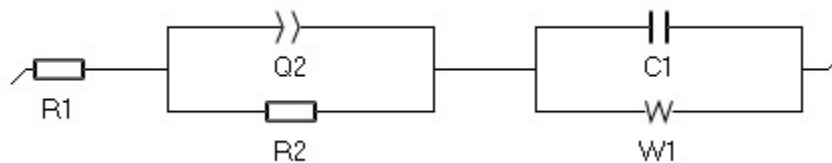


Figure S6. Equivalent circuit of the ASC device.

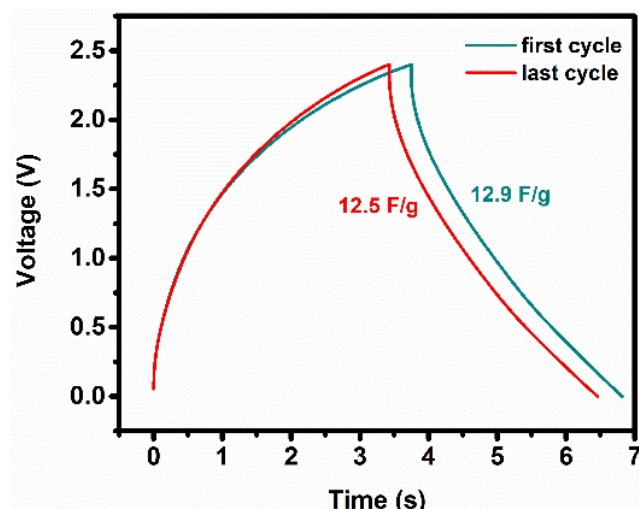


Figure S7. GCD curves of the first and last cycles of long-term stability test.

References

- [1] J.H. Kim, K. Zhu, Y. Yan, C.L. Perkins, A.J. Frank, Microstructure and pseudocapacitive properties of electrodes constructed of oriented NiO-TiO₂ nanotube arrays, *Nano Lett.* 10 (2010) 4099–4104. <https://doi.org/10.1021/nl102203s>.
- [2] N.K. Allam, C.A. Grimes, Formation of vertically oriented TiO₂ nanotube arrays using a fluoride free HCl aqueous electrolyte, *J. Phys. Chem. C.* 111 (2007) 13028–13032. <https://doi.org/10.1021/jp073924i>.
- [3] F.F. Narges, S. Tohru, A novel method for synthesis of titania nanotube powders using rapid breakdown anodization, *Chem. Mater.* 21 (2009) 1967–1979. <https://doi.org/10.1021/cm900410x>.
- [4] B. D. Cullity, R. Smoluchowski, *Phys. Today* 1957, 10, 50–50